Volume xxx, (1999) number yyy pp. 000–000

Reflectance Models with Fast Importance Sampling

László Neumann, Attila Neumann, László Szirmay-Kalos

Department of Control Engineering and Information Technology,
Technical University of Budapest,
Budapest, Műegyetem rkp. 11, H-1111, HUNGARY
Email: szirmay@iit.bme.hu, neumann@mail.datanet.hu

Abstract
We introduce a physically plausible mathematical model for a large class of BRDFs. The new model is as simple as the well-known Phong model, but eliminates its disadvantages. It gives a good visual approximation for many practical materials: coated metals, plastics, ceramics, retro-reflective paints, anisotropic and retro-reflective materials, etc. Because of its illustrative properties it can be used easily in most commercial software and because of its low computational cost it is practical for virtual reality. The model is based on a special basic BRDF definition, which meets the requirements of reciprocity and of energy conservation. Then a class of BRDFs is constructed from this basic BRDF with different weight functions. The definition of such weight functions requires the user to specify the profile of the highlights, from which the weight function is obtained by derivation. It is also demonstrated how importance sampling can be used with the new BRDFs.
Keywords: *Rendering, reflection models, BRDF, albedo, anisotropy, retro-reflective models, coated metals, energy mirror, Monte-Carlo quadrature, importance sampling.*

1. Introduction

A central problem in photorealistic rendering is the study of the optical material models characterised by *Bi-directional Reflectance Distribution Functions*, or BRDFs.

BRDF models can be classified according to how they correspond to the real physical phenomenon of light-surface interaction.

Global illumination algorithms require that the BRDFs do not violate physics. Such shading models must satisfy both reciprocity and energy balance, and are called *physically plausible*[1]. Physically plausible models can be constructed empirically using simple functions and enforcing properties of the reciprocity and energy balance, or they can be derived from more detailed physical models describing the microstructure of surfaces or the scattering of electromagnetic waves[2].

The classical Lambert model of diffuse reflection and the Torrance-Sparrow model[3] of specular reflection are physically founded. Other physically based models used so far are the Cook-Torrance[4] and He-Torrance[5] models, which are good approximations for metals and plastics but are very expensive computationally. The Cook-Torrance model has been generalised for anisotropic surfaces by Kajiya[6]. The Cook-Torrance model has also been simplified and made appropriate for practical implementations by Ward[7] and Schlick[20].

The original Phong[8], Phong-Blinn[9] and Whitted[10] models, on the other hand, are empirical models. These models are not physically plausible since they do not fulfil the law of reciprocity and the principle of the conservation of energy. The physically plausible Oren-Nayar model[11] characterises different materials with an appropriate retro-reflective component, including ceramics, walls, foams, etc. Painted coatings are often fitted to the Beard-Maxwell empirically based model[12]. The NIST database also applies this model to represent measurement data. Recently, Lafortune et.al.[13] proposed the combination of general cosine models to obtain a versatile family of BRDFs.

Based on the preliminary version of this paper[14], Tobler et.al.[15] proposed a new BRDF that is particularly good for producing artistic contour effects.

During rendering, the BRDF models are usually used for two different purposes. On the one hand, in local illumination formulae the output radiance in a direction is computed from the incident radiance and from the surface orientation, which requires the evaluation of the BRDF for a single view vector and light vector pair. On the other hand, to improve Monte-Carlo random walk methods by applying importance sampling, directions should be generated that follow a probability density of the BRDF multiplied by a cosine function.

A practically useful BRDF must support both tasks. Unfortunately, physically based BRDFs contain many complex formulae, thus not only applying accurate importance sampling is hopeless, but even their simple evaluation is rather time consuming.

This is one reason why the Phong model is still in common use despite of its deficiencies. In global illumination algorithms, it is usually modified to satisfy reciprocity[16, 1] and to allow simple importance sampling[17]. The main disadvantage of the physically plausible Phong model is evident for "grazing angles" where it becomes dark. If the exponent parameter is high, this darkening is true from two different aspects. At grazing angles both the radiance and the total reflected power sharply decrease. The missing power becomes noticeable in images generated by global illumination algorithms.

This paper intends to develop a class of BRDF models. The proposed models are physically plausible, but not physically based. It can be viewed as a mathematical construction that is simple to compute and is particularly efficient for importance sampling.

Specific members of the new class can be defined in a new way. The computational cost of the new BRDFs is comparable to that of the Phong model. The model is able to approximate the visual properties of metals, plastics, reflective, retro-reflective and anisotropic materials.

2. Basic BRDF

The complex models to be proposed by this paper are based on a simple, elementary BRDF model. This *basic BRDF* is just a mathematical tool, we do not intend to use it directly for rendering.

In the formulae the classical notations are used: $\mathbf{L}$ and $\mathbf{V}$ are the unit vectors to the light source and to the viewpoint, $\mathbf{N}$ is the unit normal vector of the surface element. The $\mathbf{L}'$ and $\mathbf{V}'$ vectors are the results of mirroring the $\mathbf{L}$ and $\mathbf{V}$ vectors across the normal vector $\mathbf{N}$. The subscript P indicates the orthogonal projection of the given unit vectors - or their endpoints - onto the base plane as shown in figure 1.

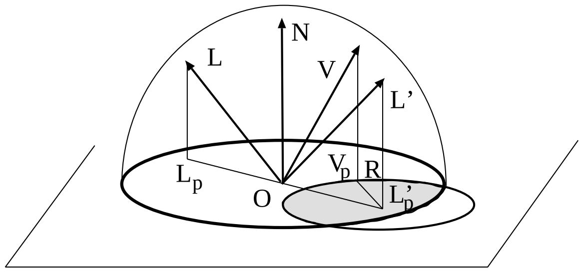

Figure 1: *Geometry of the BRDF definition*

The basic BRDF is based on simple geometric constructs, namely on circles on the base plane. Before giving the definition of the proposed basic BRDF, two notations are introduced.

Firstly, let $C(\mathbf{L}'_P, R)$ denote the common part of two circles, namely the unit circle with centre in $\mathbf{O}$ called the base circle and the circle of radius R and centre $\mathbf{L}'_P$.

Secondly, let the $m(\mathbf{L},\mathbf{V})$ metric be the distance of the $\mathbf{L}'_P$ and $\mathbf{V}_P$ points. It can be shown that

$$m(\mathbf{L},\mathbf{V}) = |\mathbf{V}_P - \mathbf{L}'_P| = |\mathbf{h} - (\mathbf{N}\cdot\mathbf{h})\mathbf{N}| \qquad (1)$$

where $\mathbf{h} = \mathbf{L}+\mathbf{V}$. It must be emphasised that $\mathbf{h}$ is not the same as the half-way unit vector denoted usually by $\mathbf{H}$, since $\mathbf{h}$ is *not normalised*.

Note that function m is symmetric, that is

$$m(\mathbf{L},\mathbf{V}) = m(\mathbf{V},\mathbf{L})$$

since the distance of $\mathbf{L}'_P$ and $\mathbf{V}_P$ is the same as the distance between $\mathbf{V}'_P$ and $\mathbf{L}_P$.

Using these notations, the basic BRDF corresponding to parameter R ($0 \le R \le 2$) is defined by:

$$f_r^*(R,\mathbf{L},\mathbf{V}) = \begin{cases} c(R) \text{ if } m(\mathbf{L},\mathbf{V}) \le R, \\ 0 \text{ otherwise.} \end{cases} \qquad (2)$$

where $c(R)$ is a constant depending on R.

Note that $m(\mathbf{L},\mathbf{V}) \le R$ means that the projection of $\mathbf{V}$ is in the circle of radius R, which is centred by the mirror of projection $\mathbf{L}$, i.e.

$$\mathbf{V}_P \in C(\mathbf{L}'_P, R).$$

Thus the BRDF also depends on R, which is shown by including it as the first parameter. The star character is to emphasise the fact that this is a basic BRDF from which other BRDFs will be constructed.

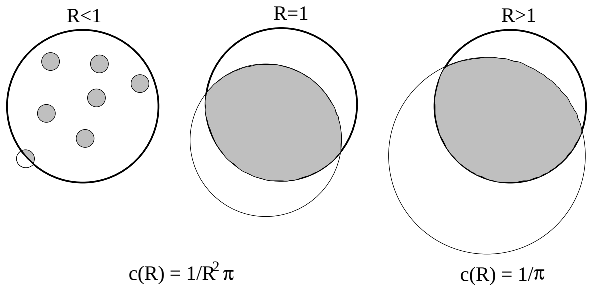

Figure 2: *Possible relations to the base circle*

The basic BRDF is a constant $c(R)$ if the projection of the mirroring of $\mathbf{L}$ onto the centre of the directional sphere and the projection of $\mathbf{V}$ are not further than R.

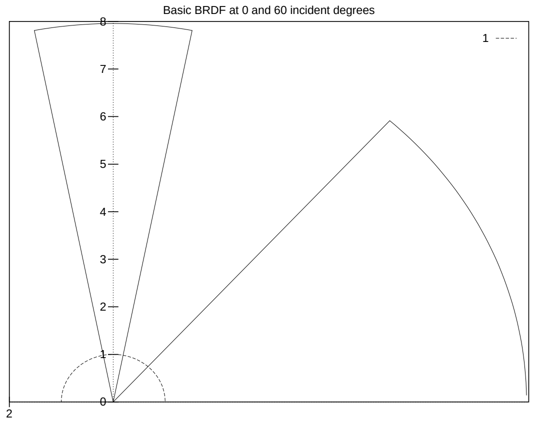

Figure 3: *Basic BRDF for $R = 0.2$*

The computation of the basic BRDF function is quite simple:

BasicBRDF$(R, \mathbf{V}, \mathbf{N}, \mathbf{L})$
  $\mathbf{h} = \mathbf{L} + \mathbf{V}$
  $m^2 = |\mathbf{h} - (\mathbf{N} \cdot \mathbf{h})\mathbf{N}|^2$
  if $(m^2 \leq R^2)$ **then return** $c(R)$
  else **return** 0
end

2.1. Reciprocity

The basic BRDF is reciprocal, which is represented by identity

$$f_r^*(R, \mathbf{L}, \mathbf{V}) = f_r^*(R, \mathbf{V}, \mathbf{L})$$

since according to definition (2) it is equivalent to

$$m(\mathbf{L}, \mathbf{V}) = m(\mathbf{V}, \mathbf{L}).$$

2.2. Energy conservation

2.2.1. Albedo function

The power reflected into the half-space from the point light source of unit irradiance situated in direction $\mathbf{L}$ is called the direction-dependent *albedo*, or the *directional hemiospherical reflectance*:

$$a(\mathbf{L}) = \int_{\Omega} f_r(\mathbf{L}, \mathbf{V})\ (\mathbf{N} \cdot \mathbf{V})\ d\omega_{\mathbf{V}}. \tag{3}$$

To satisfy energy conservation, the reflected power cannot exceed the incoming power, that is

$$a(\mathbf{L}) \leq 1. \tag{4}$$

The albedo of the basic BRDF can be easily determined. In formula (3) the multiplication with $(\mathbf{N} \cdot \mathbf{V}) = \cos \omega_{\mathbf{V}}$ corresponds to the *projection onto the base plane*. Thus, according to definitions (2) and (3) the albedo is proportional to the area of $C(\mathbf{L}'_P, R)$, that is

$$a_R(\mathbf{L}) = c(R) \cdot \mathrm{Area}(C(\mathbf{L}'_P, R)). \tag{5}$$

The area of $C(\mathbf{L}'_P, R)$ is maximum when $\mathbf{L} = \mathbf{N}$, i.e. $\mathbf{L}'_P = \mathbf{O}$. If $R < 1$, this means that the circle is not truncated. If $R \geq 1$, then the common part coincides with the base circle. Since

$$\mathrm{Area}(C(\mathbf{L}'_P, R)) \leq \mathrm{Area}(C(\mathbf{O}, R)), \tag{6}$$

if in equation (2) we choose

$$c(R) = \frac{1}{\mathrm{Area}(C(\mathbf{O}, R))} = \frac{1}{(\pi \cdot \min(1, R^2))}, \tag{7}$$

then the albedo

$$a_R(\mathbf{L}) = \frac{\mathrm{Area}(C(\mathbf{L}'_P, R))}{\mathrm{Area}(C(\mathbf{O}, R))} \tag{8}$$

will not exceed 1, that is, the basic BRDF will conserve energy.

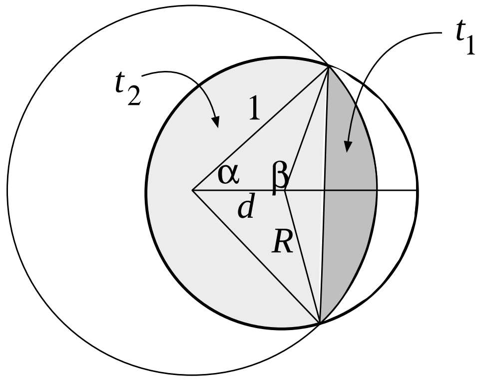

Figure 4: *Computation of the intersection of two circles*

To compute Area$(C(\mathbf{L}'_P, R))$, the intersection of two circles must be determined. Let the distance of the two circles be d. If $d < 1 - R$ or $d > 1 + R$, then the solution is trivial. For the intersecting case, we can use the following formulae that uses the notation of figure 4:

$$\text{Area}(C(\mathbf{L}'_P, R)) = t_1 + t_2 =$$

$$1 \cdot (\alpha - \cos\alpha \cdot \sin\alpha) + R^2 \cdot (\beta - \cos\beta \cdot \sin\beta). \quad (9)$$

The angle α and β can, in turn, be determined using the theorem of cosine angles:

$$\begin{aligned} d^2 + 1^2 - 2d \cdot \cos\alpha &= R^2 \\ d^2 + R^2 - 2d \cdot R \cdot \cos\beta &= 1. \end{aligned} \quad (10)$$

The direction-dependent albedo of the basic BRDF will reach the imposed maximum of 1 for vertical illumination, i.e. for $\mathbf{L} = \mathbf{N}$.

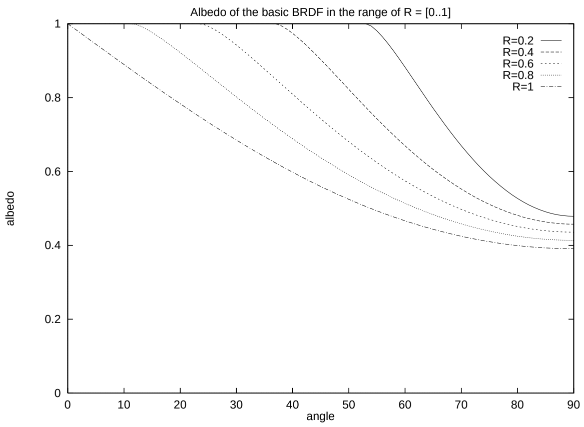

Figure 5: *Albedo of the basic BRDF for small R values ($R \le 1$)*

When $R < 1$, then the albedo equals to the ratio of the area of the possibly truncated circle and the area of the complete circle of radius R. For $R \ge 1$ it is the ratio of the area of the possibly truncated base circle and the area of the whole base circle (π). Thus, we always have $a_R(\mathbf{N}) = 1$, furthermore it is easy to show that

$$0.391 < \frac{2}{3} - \frac{\sqrt{3}}{2\pi} \le a_R(\mathbf{L}) \le 1$$

holds. The minimum point is at horizontal illumination ($(\mathbf{N} \cdot \mathbf{L}) = 0$) and for $R = 1$.

For small values of R, the albedo is generally 1, and even at the margins of the base circle it hardly decreases under half. This is due to the fact that in this case the circle is generally not truncated, only for illumination at grazing angles.

The $R = 0$ situation is the marginal case corresponding to a special mirror. In this case $C(R)$ becomes a Dirac-delta function.

The $R = 2$ case corresponds to the ideal diffuse model, where also $a(\mathbf{L}) \equiv 1$.

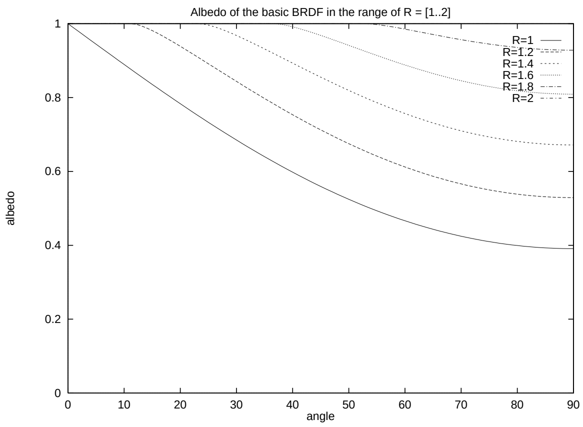

Figure 6: *Albedo of the basic BRDF for large R values ($1 \le R \le 2$)*

2.2.2. Mean albedo

In addition to the direction-dependent albedo defined by equation (3), we can also introduce the notion of the *mean albedo*. This direction-independent and dimensionless value is equal to the "reflectivity" for diffuse materials.

For non-diffuse materials, it can be defined as the weighted mean value of direction-dependent albedos:

$$a_{\text{mean}} = \frac{1}{\pi} \cdot \int_{\Omega} a(\mathbf{L})\ (\mathbf{N} \cdot \mathbf{L})\ d\omega_{\mathbf{L}}, \quad (11)$$

where $\mathbf{L}$ is the running vector of the directional hemisphere and the weighting factor is $(\mathbf{N} \cdot \mathbf{L}) = \cos\omega_{\mathbf{L}}$.

In the case of uniform illumination on the half-space, the value of the mean albedo is equal to the ratio of the reflected and the incident power. Figure 7 illustrates the values of a_{mean} for the basic BRDFs as a function of R. The mean albedo is minimal at $R = 1$.

The BRDF and the albedo characterise a material from two different aspects. The BRDF is used to describe the "reflected radiance" and it is a scalar which depends on both $\mathbf{L}$ and $\mathbf{V}$. The albedo depending only on direction $\mathbf{L}$ serves for the description of the "reflected power". The mean albedo (which does not depend on $\mathbf{L}$ and $\mathbf{V}$) characterises the average reflectivity of the BRDF.

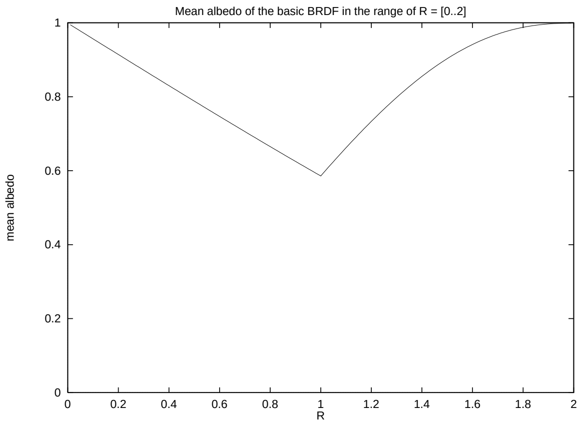

Figure 7: *Mean albedo of the basic BRDF*

Examining these characteristics, we can see the essential difference between the behaviour of the ideal mirror obtained by the new BRDF and that obtained as a limit case from the $(\mathbf{N}\cdot\mathbf{H})^n$ Phong-Blinn model without diffuse component[18].

For the ideal metal mirror, both the mean and the direction dependent albedos are 1, that is $a_{\rm mean} = 1$ and $a(\mathbf{L}) \equiv 1$.

However, for the "Phong-mirror", which is the result of letting n go to infinity, we have $1 \geq a(\mathbf{L}) \geq 0$ and $a_{\rm mean} = 0.5$. In the case of a Phong mirror, the reflected energy tends to zero for grazing angles.

The mirror case of the new model is not equivalent to a metal mirror since at grazing angles the metallic mirrors reflect the total energy by increasing the BRDF by a factor of $1/(\mathbf{N}\cdot\mathbf{L})$, while in the new model the BRDF is constant and the solid angle of the reflectance is increased by $1/(\mathbf{N}\cdot\mathbf{L})$. Thus the new model is a ideal "energy mirror" but not ideal "radiance mirror" for higher incident angles.

2.3. Importance sampling

Suppose that we want to calculate the radiance of a point in direction $\mathbf{V}$ due to the illumination of the scene. The input and output *radiances* $[\mathrm{Wm}^{-2}\mathrm{sr}^{-1}]$ are denoted by $L^{\rm in}$ and $L^{\rm out}$, respectively. The radiance in the viewing direction $\mathbf{V}$ is:

$$L^{\rm out}(\mathbf{V}) = \int_{\Omega} L^{\rm in}(\mathbf{L})\ f_r(\mathbf{L},\mathbf{V})\ (\mathbf{N}\cdot\mathbf{L})\ d\omega_{\mathbf{L}}. \quad (12)$$

This integral can be approximated by the Monte-Carlo method. Using importance sampling to reduce the variance, the incoming $\mathbf{L}_1, \mathbf{L}_2, \ldots, \mathbf{L}_M$ directions are not uniformly distributed, but their probability density distribution function is at least approximately proportional to the integrand. Since $L^{\rm in}(\mathbf{L})$ is usually not known a-priori, we can sample $\mathbf{L}$ with probability proportional to the

$$R(\mathbf{L},\mathbf{V}) = f_r(\mathbf{L},\mathbf{V})\ (\mathbf{N}\cdot\mathbf{L})$$

weighted BRDF function. This function has an interesting illustrative content, according to the "inverse situation". If there were a light source in the viewing direction, then the distribution of the energy on the half-space after the reflection would follow the function R.

Function $R\cdot d\omega_{\mathbf{L}}$ also defines the conditional probability that a photon is reflected into the solid angle $d\omega_{\mathbf{L}}$ given that it comes from $\mathbf{V}$ [19].

Due to the fact that f_r is reciprocal, we have:

$$a(\mathbf{V}) = \int_{\Omega} f_r(\mathbf{L},\mathbf{V})\ (\mathbf{N}\cdot\mathbf{L})\ d\omega_{\mathbf{L}}, \quad (13)$$

which is exactly the value of the albedo function in viewing direction $\mathbf{V}$. For sampling of $\mathbf{L}_1, \mathbf{L}_2, \ldots, \mathbf{L}_M$ directions, we have to use the

$$d_{\mathbf{V}}(\mathbf{L}) = \frac{f_r(\mathbf{L},\mathbf{V})\cdot(\mathbf{N}\cdot\mathbf{L})}{a(\mathbf{V})}\ d\omega_{\mathbf{L}} \quad (14)$$

probability density function. The approximation of the integral in equation (12) is:

$$L^{\rm out}(\mathbf{V}) = a(\mathbf{V})\cdot E\left[L^{\rm in}(\mathbf{L})\right] \approx \frac{a(\mathbf{V})}{M}\cdot\sum_{k=1}^{M} L^{\rm in}(\mathbf{L}_k). \quad (15)$$

In the case of isotropic BRDFs the albedo functions can be tabulated in a one-dimensional table. When calculating multiple interreflections, the main computational problem is the generation of the directions from equation (14) following distribution $d_{\mathbf{V}}$.

2.4. Importance sampling for the basic BRDF

2.4.1. Sampling in special cases

For the introduced basic BRDFs, we can easily generate directions with a distribution of equation (14).

Let us consider first a circle of radius $R < 1$ and assume that this circle does not intersect the base circle. In this case $C(\mathbf{V}'_P, R)$ is identical with the circle with centre in $\mathbf{V}'_P$ and of radius R. The value of the albedo is 1 because the circle is not truncated.

Let us generate M number of 2D points inside this circle with a uniform distribution. These will be the $(\mathbf{L}_k)_P$ $(k = 1, \ldots, M)$ projection points in the plane of projection. Since the projection automatically includes the "cosine" factor in $d(\mathbf{L})$, re-projecting these points onto the unit hemisphere's surface, we obtain the $\mathbf{L}_1, \mathbf{L}_2, \ldots, \mathbf{L}_M$ directions of the desired distribution.

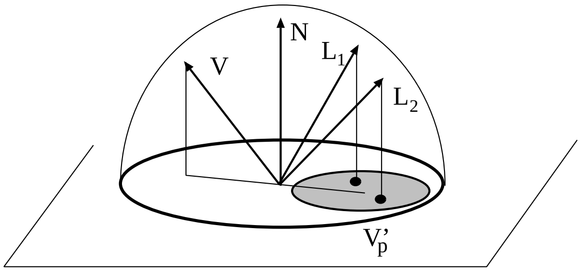

Figure 8: *Sampling when $R < 1$ and the circles do not intersect*

For a given unit viewing vector $\mathbf{V}$, the projection on the base plane and the mirroring are realised in the following way:

$$\mathbf{V}'_P = -\mathbf{V}_P = -(\mathbf{V} - (\mathbf{N} \cdot \mathbf{V})\mathbf{N}). \tag{16}$$

The formula for re-projecting the $\mathbf{L}_P$ sample point which is inside the circle of centre $\mathbf{V}'_P$ and of radius R onto the hemisphere is:

$$\mathbf{L} = \mathbf{L}_P + \sqrt{1 - (\mathbf{L}_P \cdot \mathbf{L}_P)} \cdot \mathbf{N}. \tag{17}$$

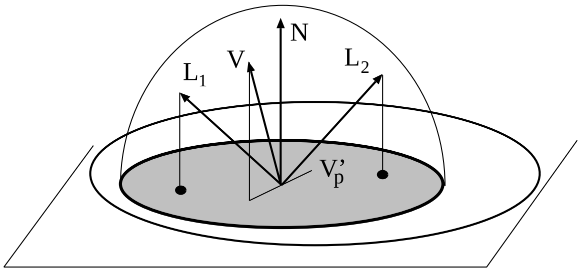

Figure 9: *Sampling when $R \geq 1$ and the circles do not intersect*

The situation is similar if $R > 1$ and the circle contains the complete unit base circle. Now the uniformly distributed points can be generated on the whole base circle. This case corresponds to the generation of directions following a "cosine distribution" for diffuse materials.

2.4.2. Generating uniformly distributed points in a circle

To generate uniformly distributed points inside a circle, we can either use an area preserving mapping of the square onto the circle, or apply rejection sampling. In rejection sampling the points are generated in a square that encloses the circle and those points that are outside the circle are ignored.

2.4.3. Sampling in the general case

In the cases discussed so far, the domain where the sample points are generated was a complete circle and the value of the albedo was 1. In the general case the $C(\mathbf{V}'_P, R)$ region is the common part of two circles. To realise importance sampling, we have to generate uniformly distributed points inside this region.

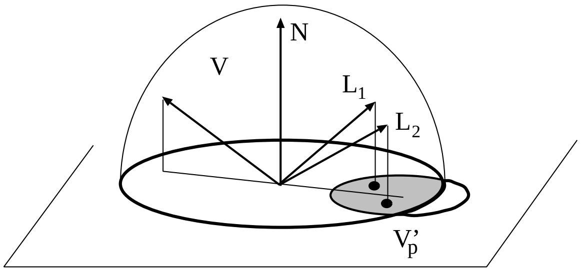

Figure 10: *Sampling when the circles intersect*

To solve this problem, *rejection sampling* can be applied. It means that uniform samples are generated in one of the circles and then checked whether or not the other circle contains this sample. If it does not, the sample is rejected and a new sample is generated.

To reduce the number of rejected samples, the smaller circle is worth selecting as a domain for sample generation and the bigger as the region of rejection sampling.

The following subroutine finds an $\mathbf{L}$ sample from direction $\mathbf{V}$ using a basic BRDF of parameter R, and also provides the albedo to weight the radiance obtained using direction $\mathbf{L}$:

DOUBLE GenerateDirectionWithBasicBRDF($R, \mathbf{V}, \mathbf{N}, \mathbf{L}$)
    $\mathbf{V}'_P = -(\mathbf{V} - (\mathbf{N} \cdot \mathbf{V})\mathbf{N})$
    found = TRUE
    repeat
      if $R < 1$ **then**
        Generate point $\mathbf{L}_P$ in $C(\mathbf{V}'_P, R)$
        if $\mathbf{L}_P$ is outside $C(\mathbf{O}, 1)$ **then** found = FALSE
      else
        Generate point $\mathbf{L}_P$ in $C(\mathbf{O}, 1)$
        if $\mathbf{L}_P$ is outside $C(\mathbf{V}'_P, R)$ **then** found = FALSE
      endif
    until found
    $\mathbf{L} = \mathbf{L}_P + \sqrt{1 - (\mathbf{L}_P \cdot \mathbf{L}_P)} \cdot \mathbf{N}$
    $a = C(\mathbf{V}'_P, R)/(\pi \cdot \min(1, R^2))$
    return a
end

2.4.4. Sampling with Russian roulette

In the case of highly reflective materials R is small and thus $C(\mathbf{V}'_P, R)$ is typically a complete circle. The computation of the common part of two circles is required only at the margins.

For other materials, truncation of the circles must be considered several times. However, if we use the Russian roulette, we have to check only whether or not the points are inside the circle, the albedo (the area of the common part) should not be computed explicitly. Let

$$C_{\min}(\mathbf{V}'_P, R) = \begin{cases} C(\mathbf{V}'_P, R), & \text{if } R < 1, \\ C(\mathbf{O}, 1), & \text{otherwise.} \end{cases} \tag{18}$$

Let us generate in the $C_{\min}(\mathbf{V}'_P, R)$ region exactly M uniformly distributed 2D points. Now, the weighting factor of $(\mathbf{L}_k)_P$ $(k = 1, \ldots, M)$ will be 0 or 1 (i.e. accepted or rejected) according to whether or not the point is inside the "other circle" too. The approximation of the half-space integral is:

$$L^{\text{out}}(\mathbf{V}) = E\left[L^{\text{in}}(\mathbf{L})\right] \approx \frac{1}{M} \cdot \sum_{k=1}^{M} L^{\text{in}}(\mathbf{L}_k), \tag{19}$$

where only the accepted points are considered in the sum, that is, which have a weighting factor of 1. This means that the number of terms can be at most M, but is often less. This method is somewhat simpler, but its variance is not the possible minimum because it does not carry out the exact importance sampling. The weight factors of the elementary rays are 0 or 1, only their expected value is equal to the $a_R(\mathbf{V})$ albedo.

The algorithm that generates either direction $\mathbf{L}$ from direction $\mathbf{V}$, or reports that the sample should be rejected by returning a zero value is the following:

BOOL GenerateDirectionWithBasicBRDF$(R, \mathbf{V}, \mathbf{N}, \mathbf{L})$
  $\mathbf{V}'_P = -(\mathbf{V} - (\mathbf{N} \cdot \mathbf{V})\mathbf{N})$
  if $R < 1$ **then**
    Generate point $\mathbf{L}_P$ in $C(\mathbf{V}'_P, R)$
    if $\mathbf{L}_P$ is outside $C(\mathbf{O}, 1)$ **then return** 0
  else
    Generate point $\mathbf{L}_P$ in $C(\mathbf{O}, 1)$
    if $\mathbf{L}'_P$ is outside $C(\mathbf{V}'_P, R)$ **then return** 0
  endif
  $\mathbf{L} = \mathbf{L}_P + \sqrt{1 - (\mathbf{L}_P \cdot \mathbf{L}_P)} \cdot \mathbf{N}$
  return 1
end

3. Mixture of basic BRDFs

3.1. General description

The basic BRDF is not a realistic material model by itself, but only a mathematical construction since it is discontinuous (figure 3). Therefore we intend to create real BRDFs using a mixture of the basic ones. Let the weighting function be $p(R)$ that is expected to be "normalised" ($\int p(R) dR = 1$).

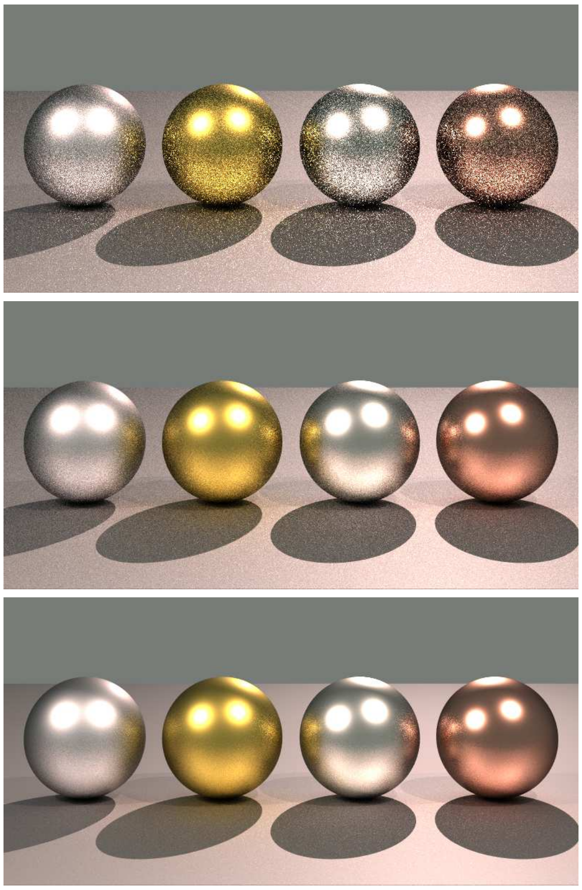

Figure 11: *Metallic spheres generated by Monte-Carlo ray tracing with 50 samples per pixel (top: importance sampling according to the cosine angle only (51 min); middle: Russian roulette based importance sampling of section 2.4.4 (46 min); bottom: normal importance sampling of section 2.4.3 (54 min)*

The *mixture BRDF* is then:

$$f_r(\mathbf{L}, \mathbf{V}) = \int_0^2 p(R) \cdot f_r^*(R, \mathbf{L}, \mathbf{V}) \, dR. \tag{20}$$

Weighting function $p(R)$ can be considered as a probability density function of one variable in the $0 \leq R \leq 2$ interval.

The mixture BRDFs evidently meet the requirements of reciprocity and energy conservation. So the BRDFs are physically plausible models if their value is non-negative. A sufficient but not necessary condition is that the weighting function is non-negative.

The singularities of Dirac-delta type cases must be examined separately, namely when the integral of $p(R)$ in the respective point is a finite, non-zero value, and $p(R)$ is "infinite".

Two types of singularities are important in BRDF modelling. The $R = 0$ case corresponds to a special ideal mirror, and $R = 2$ corresponds to the ideal diffuse model. Separating these, we have:

$$\int_0^2 p(R)dR = p_{\text{Mirror}} + p_{\text{Diffuse}} + \int_{+0}^{2-0} p(R)\ dR = 1 \quad (21)$$

3.2. Albedo for a given $p(R)$ function

Since mixing is a linear operation, the albedo a^p and the mean albedo a^p_{mean} of the mixture BRDF can be computed as follows:

$$a^p(\mathbf{L}) = \int_0^2 p(R) \cdot a_R(\mathbf{L})\ dR, \quad (22)$$

$$a^p_{\text{mean}} = \int_0^2 p(R) \cdot (a_R)_{\text{mean}} dR. \quad (23)$$

According to equation (21) for the albedos of the mirror and of the Lambertian model, we have:

$$a_{\text{Mirror}} = p_{\text{Mirror}}, \qquad a_{\text{Diffuse}} = p_{\text{Diffuse}}. \quad (24)$$

4. Modified importance sampling for a given $p(R)$

4.1. Reducing the general case to basic BRDFs

Using equations (12) and (20), we transform the half-space integral into a double integral and then reverse the order of integration:

$$L^{\text{out}}(\mathbf{V}) = \int_\Omega L^{\text{in}}(\mathbf{L})\ f_r(\mathbf{L},\mathbf{V})\ (\mathbf{N}\cdot\mathbf{L})\ d\omega_{\mathbf{L}} =$$

$$\int_\Omega L^{\text{in}}(\mathbf{L}) \cdot \left[\int_0^2 p(R)\ f_r^*(R,\mathbf{L},\mathbf{V})\ dR\right] (\mathbf{N}\cdot\mathbf{L})\ d\omega_{\mathbf{L}} =$$

$$\int_0^2 p(R) \cdot \left[\int_\Omega L^{\text{in}}(\mathbf{L})\ f_r^*(R,\mathbf{L},\mathbf{V})\ (\mathbf{N}\cdot\mathbf{L})\ d\omega_{\mathbf{L}}\right] dR =$$

$$\int_0^2 p(R) \cdot L_R^{\text{out}}(\mathbf{V})\ dR. \quad (25)$$

This integral is approximated by a sum using Monte-Carlo quadrature. For the calculation of the required R_k values, we apply importance sampling according to the $p(R)$ function. Using the approximate value of the integral (12), we have:

$$L^{\text{out}}(\mathbf{V}) = \int_0^2 p(R) \cdot L_R^{\text{out}}(\mathbf{V})\ dR \approx \frac{1}{M} \cdot \sum_{k=1}^{M} L^{\text{in}}_{R_k}(\mathbf{V}), \quad (26)$$

similarly to equation (25), with the exception that here each incoming direction is represented by a different radius R_k.

Let the cumulative probability distribution function of p be the following function:

$$F(R) = \int_0^R p(t)\ dt, \quad (0 \le R \le 2, \quad 0 \le F(R) \le 1). \quad (27)$$

In practice, we may calculate F in a closed form, or using numerical methods. Importance sampling requires the inverse of F, which is usually computed numerically and the resulting values are stored in a sufficiently large one-dimensional array.

The algorithm of generating a direction $\mathbf{L}$ to direction $\mathbf{V}$ is as follows:

```
BOOL GenerateDirectionWithMixtureBRDF(V, N, L)
    Generate a random value r in [0, 1]
    R = F^{-1}(r)
    return GenerateDirectionWithBasicBRDF(R, V, N, L)
end
```

5. Generalisation of the basic BRDF

5.1. Generalisation of the $\mathbf{L} \to \mathbf{L}'$ mirroring transformation

The $\mathbf{L}'$ vector in definition (2) was obtained from the original $\mathbf{L}$ vector by mirroring. Instead of mirroring, basic BRDFs can be defined using other $\mathbf{L} \to T(\mathbf{L})$ transformations too. To fulfil the requirement of reciprocity, the $T(\mathbf{L})$ transformation has to satisfy the following identity:

$$T(T(\mathbf{L})) = \mathbf{L}. \quad (28)$$

This requirement is satisfied by mirroring since mirroring two times gives back the original point.

Another trivial transformation is the identity, that is $T(\mathbf{L}) = \mathbf{L}$.

5.2. The retro-reflective model

For the $T(\mathbf{L}) = \mathbf{L}$ transformation, the $m(\mathbf{L}, \mathbf{V})$ metric from definition (2) becomes:

$$m(\mathbf{L}, \mathbf{V}) = |\mathbf{L}_P - \mathbf{V}_P| = |\mathbf{g} - (\mathbf{N} \cdot \mathbf{g})\mathbf{N}|, \qquad (29)$$

where $\mathbf{g} = \mathbf{L} - \mathbf{V}$. For such models, the radiance of the reflected light is maximum in the incidence direction. This model is called the *retro-reflective model*. In practice, materials exhibiting such properties are the beaded screens or the signal paints used on the highways. The marginal cases of this retro-reflective model are those mirror-constructions which are used in laser-based telemeters that behave practically as ideal mirrors, but reflect exactly in the incident direction.

5.3. Generalisation of the metric

In definition (2) the $m(\mathbf{L}, \mathbf{V})$ metric was an Euclidean distance in the projection plane. The metric can be generalised as follows:

$$m(\mathbf{L}, \mathbf{V}) = ||\mathbf{V}, T(\mathbf{L})||. \qquad (30)$$

In equation (30) $||\cdot,\cdot||$ is an arbitrary metric for two unit vectors on the hemisphere. For the Euclidean metric on the base plane and for basic BRDFs defined in equation (2), we have:

$$||\mathbf{V}, T(\mathbf{L})|| = |\mathbf{V}_P - T(\mathbf{L})_P|. \qquad (31)$$

5.4. Anisotropic models

The use of anisotropic models can often substantially improve realism in rendering, especially in the case of metals[6, 20]. Formula (31) provides useful generalisation possibilities for practice. Using an “elliptic norm” on the base plane, anisotropic BRDFs are obtained. Let us define an orthonormal co-ordinate system on the surface element representing the given BRDF, by considering the $(\mathbf{u}, \mathbf{v})$ vectors which are perpendicular to each other and to the $\mathbf{N}$ unit normal vector too. The metric m can be defined as follows:

$$m(\mathbf{L}, \mathbf{V}) = \sqrt{\left(\frac{B}{A} \cdot (\mathbf{z} \cdot \mathbf{u})\right)^2 + (\mathbf{z} \cdot \mathbf{v})^2}, \qquad (32)$$

where $\mathbf{z} = \mathbf{V}_P - T(\mathbf{L})_P$ and $B/A \leq 1$ is the ratio of the axes of the ellipse, and the major and the minor axis of the ellipse are taken along vectors $\mathbf{u}$ and $\mathbf{v}$, respectively. This metric m contracts the distance component along vector $\mathbf{u}$. When $B/A = 1$, we have the same case as in equation (1).

Let $E(\mathbf{Q}, \mathbf{v}, b)$ denote the common part of the ellipse with centre in $\mathbf{Q}$, with a minor axis of length b and of the unit base circle. In this case:

$$\mathbf{V}_P \in E(\mathbf{L}'_P, \mathbf{v}, b) \Longleftrightarrow \mathbf{L}'_P \in E(\mathbf{V}'_P, \mathbf{v}, b), \qquad (33)$$

which means that the model meets the requirement of reciprocity.

The maximum value of b is determined for that case when the $E(\mathbf{Q}, \mathbf{v}, b)$ ellipse contains the complete unit base circle, for every $\mathbf{Q}$ inside the base circle. The maximal $b = 2$ case happens for illumination which is along the minor axis and is horizontal. The value of b can be in $[0, 2]$, the length of the major axis in $[0, 2A/B]$.

Parameter b corresponds to the earlier R parameter. The elementary BRDF depends now only on b:

$$f_r^*(b, \mathbf{L}, \mathbf{V}) = \begin{cases} c(b), \text{ if } \mathbf{V}_P \in E(\mathbf{L}'_P, \mathbf{v}, b), \\ 0 \text{ otherwise.} \end{cases} \qquad (34)$$

The albedo of the BRDF in formula (34) is:

$$a_b(\mathbf{L}) = \frac{\text{Area}(E(\mathbf{L}'_P, \mathbf{v}, b))}{\text{Area}(E(\mathbf{O}, \mathbf{v}, b))}. \qquad (35)$$

The albedo is maximal for $\mathbf{L} = \mathbf{N}$. The constant in equation (34) for every value of b is taken so that for a vertical illumination the albedo function is 1.

The computation of this constant can be separated into two cases. When $b \leq B/A$, i.e. when the major axis is less than 1, the base circle contains the whole ellipse with centre $\mathbf{Q} = \mathbf{O}$. On the other hand, when the major axis is greater than 1, the intersections should be computed.

$$c(b) = \begin{cases} 1/(ab\pi), & \text{if } b \leq B/A, \\ 1/\text{Area}(E(\mathbf{O}, \mathbf{v}, b)), & \text{if } B/A < b \leq 2. \end{cases} \qquad (36)$$

In importance sampling, the anisotropic model can be used similarly to the isotropic model. Points are generated inside a circle that has radius b, then a scaling transformation is applied that transforms the circle to the ellipse.

The anisotropic model can also be used to define mixture BRDFs:

$$f_r(\mathbf{L}, \mathbf{V}) = \int_0^2 p(b) \cdot f_r^*(b, \mathbf{L}, \mathbf{V})\, db = \int_{m(\mathbf{L}, \mathbf{V})}^2 p(b) \cdot c(b)\, db \qquad (37)$$

Anisotropic models can be defined with other norms

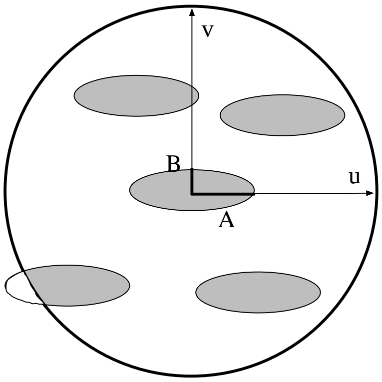

Figure 12: *Elliptical BRDFs*

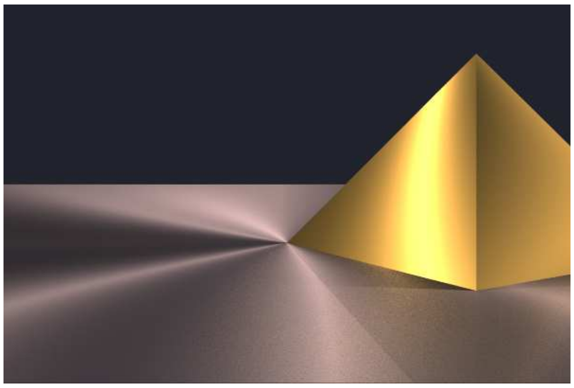

Figure 13: *A scene containing anisotropic metals*

too, for example with the p-th power norm:

$$m(\mathbf{L},\mathbf{V}) = \left[\left(\frac{B}{A}(\mathbf{z}\cdot\mathbf{u})\right)^p + (\mathbf{z}\cdot\mathbf{v}))^p\right]^{1/p} \qquad (38)$$

6. BRDF definition with a given scalar function

A BRDF maps two vector variables to a scalar value, thus always involves dimension reduction. The exact phase where the dimension reduction happens can vary in different BRDFs. The dimension reduction also means that each BRDF can be associated with equivalence classes of vector pairs, in a way that two vector pairs provide the same BRDF value if they are in the same class. In Phong-Blinn BRDFs, for example, all $\mathbf{L},\mathbf{V}$ pairs are equivalent if they have the same $\mathbf{N}\cdot\mathbf{H}$ scalar product. In the new model, the dimensional reduction takes place when computing the $m(\mathbf{L},\mathbf{V}) = |\mathbf{h} - (\mathbf{N}\cdot\mathbf{h})\mathbf{N}|$ metric.

In this section we shall examine how a BRDF can be defined with an arbitrary function of one variable and how its corresponding $p(R)$ function can be determined. Let us consider an arbitrary, non-negative $\xi(m)$ scalar function defined in the $[0,2]$ interval, which will define the shape of the reflection lobes or the characteristics of the BRDF. Using this, we define a $f_r^\xi(\mathbf{L},\mathbf{V})$ function:

$$f_r^\xi(\mathbf{L},\mathbf{V}) = \xi(m(\mathbf{L},\mathbf{V})) = \xi(m), \quad m \in [0,2] \qquad (39)$$

Function $\xi(m)$ is multiplied with an appropriate $C_{\max}$ constant in order to fulfil energy conservation requirement, thus the

$$f_r(\mathbf{L},\mathbf{V}) = f_r^{C_{\max}\xi}(\mathbf{L},\mathbf{V}) = C_{\max}\cdot f_r^\xi(\mathbf{L},\mathbf{V})$$

function will be a plausible BRDF.

Let us recall definition (20) of the mixture BRDFs. The lower limit of the integral can be modified, since according to definition (2), if $R < m(\mathbf{L},\mathbf{V})$, the value of $f_r(R,\mathbf{L},\mathbf{V})$ is zero. When $R \geq m$, its value is the $c(R)$ defined by equation (7). Thus, the following formula is equivalent to formula (20) for the definition of the mixture BRDF:

$$f_r(\mathbf{L},\mathbf{V}) = \int_{m(\mathbf{L},\mathbf{V})}^{2} p(R)\cdot f_r^*(R,\mathbf{L},\mathbf{V})\, dR =$$

$$\int_{m(\mathbf{L},\mathbf{V})}^{2} p(R)\cdot c(R)\, dR = \int_{m(\mathbf{L},\mathbf{V})}^{2} p(R)\cdot\pi\cdot\min(1,R^2)\, dR. \qquad (40)$$

Computing the derivative according to variable m, we obtain:

$$p(R) = -C_{\max}\cdot\frac{d\xi(m)}{dm}(R)\cdot\pi\cdot\min(1,R^2). \qquad (41)$$

The derivative of function ξ must be taken with a minus sign, since m is the lower limit of the integration.

The $C_{\max}$ factor should be set to make $p(R)$ a probability density and consequently the BRDF energy conserving, thus

$$\frac{1}{C_{\max}} = -\int_0^2 \frac{d\xi(m)}{dm}(R)\cdot\pi\cdot\min(1,R^2)\, dR \qquad (42)$$

for decreasing ξ functions.

The maximum of the albedo of this BRDF is 1. To obtain darker materials, the BRDF can be multiplied with a factor that is less than 1.

In a software implementing this approach ξ can be provided interactively by the user as an arbitrary curve using a graphics interface (the curve defines a one variable function). Only the ratio of the ideal mirror component (polishing) must be specified separately (see equation (21)).

Note that ξ is not required to be monotone decreasing, but the condition of non-negativity must be imposed in any case. For ξ functions having monotone increasing parts, the computation of the maximal albedo and of the normalising factor is more difficult than equation (42) and can be accomplished by numerical methods using formula (22).

6.1. Analytically integrable cases

In this section we will present some monotone decreasing ξ functions which are suitable for applications and for which the $C_{\max}$ multiplier from equation (42) can be derived analytically.

Let G be the primitive function of ξ, and H be the primitive of G (with arbitrary constants!) i.e. $G = \int \xi$ and $H = \int G$.

Then, it can be easily deduced that:

$$C_{\max} = \frac{1}{2\pi(G(1) - H(1) + H(0))}. \qquad (43)$$

This formula is true even if $\xi(2) > 0$.

6.1.1. Exponential function

This section uses the exponential function as a scalar function to define the highlight profile:

$$\xi(m) = e^{-s \cdot m}. \qquad (44)$$

The normalisation factor is

$$C_{\max} = \frac{s^2}{2\pi(1 - (1+s)e^{-s})}, \qquad (45)$$

and the BRDF is

$$f_r^{(s)}(\mathbf{L}, \mathbf{V}) = \frac{s^2}{2\pi(1 - (1+s)e^{-s})} \cdot e^{-s \cdot m}. \qquad (46)$$

Using formula (41), we can obtain the following expression for the required weighting function p:

$$p(R) = -C_{\max} \cdot \frac{d\xi(m)}{dm}(R) \cdot \pi \cdot \min(1, R^2) =$$

$$\frac{s^3 \cdot e^{-s \cdot R} \cdot \min(1, R^2)}{2(1 - (1+s)e^{-s})}. \qquad (47)$$

The probability densities, the inverse of the probability distribution functions, the albedos, and the shapes of the BRDF lobes are shown in figure 14, figure 15, figure 16 and figure 17, respectively, for different s parameters.

For $s > 10$, the model is already highly specular. A

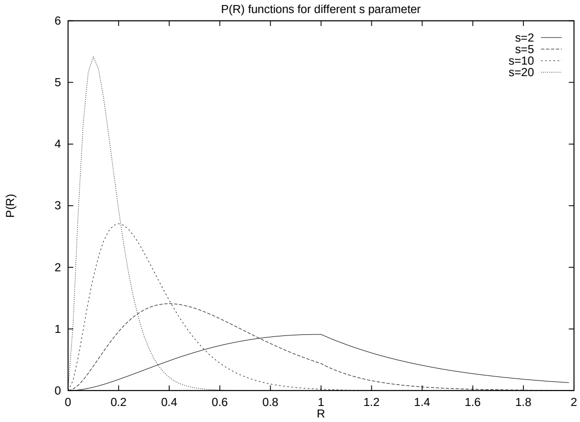

Figure 14: *Probability density function $p(R)$ for different s values*

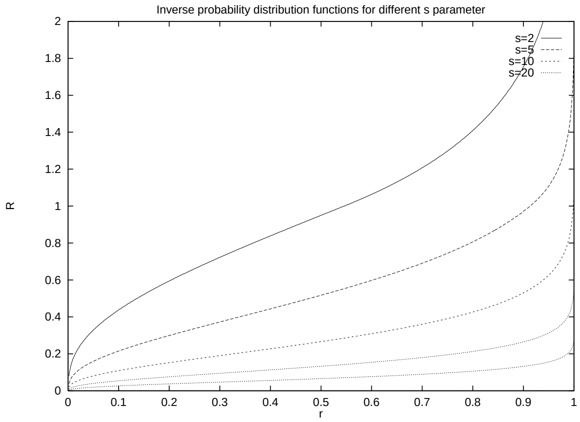

Figure 15: *Inverse of the probability distribution functions $F^{-1}(r)$ for different s values*

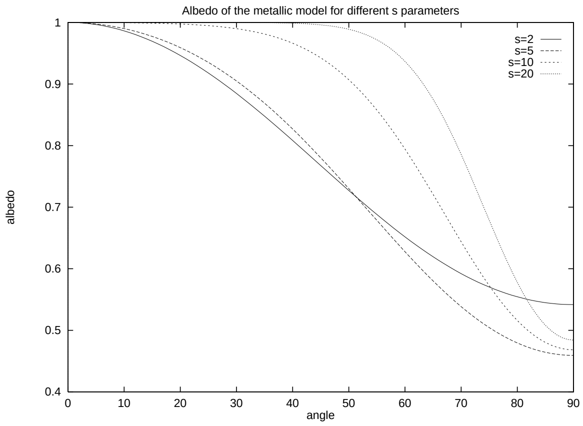

Figure 16: *Albedos of the mixed BRDFs for different s values*

very good approximation of the above formula for this parameter domain is:

$$f_r^{(s)}(\mathbf{L},\mathbf{V}) = \frac{s^2}{2\pi} \cdot e^{-s\cdot m(\mathbf{L},\mathbf{V})}. \quad (48)$$

when the corresponding p weighting function is:

$$p(R) = \frac{s^2}{2} \cdot R \cdot e^{-s\cdot R} \cdot \min(1, R^2). \quad (49)$$

Let us consider formula (40) and an $m < 1$ value:

$$f_r(\mathbf{L},\mathbf{V}) = \int_0^2 p(R) \cdot c(R)\ dR = I_{m,1} + I_{1,2} =$$

$$\pi \cdot \int_m^1 p(R) \cdot R^2\ dR + \pi \cdot \int_1^2 p(R)\ dR. \quad (50)$$

In the case of a vertical illumination we have $m \leq 1$ independently of $\mathbf{V}$, thus even for the horizontal viewing direction there will be a non-zero "diffuse part". This is component $I_{1,2}$ in equation (50) which is the integral over the $[1,2]$ interval. Thus, for the truly specular materials not only $\xi(2) = 0$ but $\xi(m) = 0$ for $m \geq 1$ must be imposed.

To illustrate this, the table 1 contains the corresponding values of the $C_{\max}$ and s parameters of the $f_r(\mathbf{L},\mathbf{V}) = C_{\max} \cdot e^{-s\cdot m}$ function, $I_{1,2}$ and $a_{\text{Diffuse}} = p_{\text{Diffuse}} = C_{\max} \cdot \pi \cdot e^{-2s}$.

7. Real materials

7.1. Metals and the new model

The BRDFs of metals increase towards infinity for grazing angles. This is due to the fact that for smooth metals the product of the BRDF and the cosine term is approximately constant, thus the incident and the outgoing radiance is approximately equal. The proposed model does not follow this behaviour since the maximum of the BRDF values is constant for any incident angle.

To further explain this, let us compare the behaviour at the limiting mirror case of the Phong, of the new model and of the real metals. Assume that the Fresnel function is approximately 1 (this is a good approximation for silver mirror, for instance), and the shininess — which is represented by s in the new model and by the exponent in the Phong model — goes to infinity. If the observer looks at the mirror perpendicularly and the illumination is also perpendicular, then both the new model and the Phong model provide the same radiance and reflected power as a real metal. However at grazing angles, while a real mirror would reflect the incoming radiance and the output power would be equal to the input power, for the Phong model both the radiance and the output power tend to zero. Interestingly, the output radiance of the new model also goes to zero at grazing angles, but the output power equals to the input power at arbitrarily close to the horizontal illumination. Thus, the new model is an energy mirror in this limiting case, but is not an ideal radiance mirror. This is "better" than the Phong model which is neither radiance nor energy mirror. The radiance mirror property means that the illumination of point light sources are reflected like real metals even at grazing angles. The energy mirror property, on the other hand, means that the distributed (e.g. skylight) illumination is reflected in a way as real metals since for uniformly distributed illumination, the perceived radiance is proportional to the albedo (equation (13).

	Phong ($n \to \infty$)	new BRDF ($s \to \infty$)	real metal mirrors
a_{mean}	1/2	1	1
$a(\theta \to 90^\circ)$	0	1	1
$L^{\text{out}}(\theta \to 90^\circ)$	0	0	L^{in}
$f_r(\theta \to 90^\circ)$	constant	constant	∞

Table 2: *Comparison the limiting case of the Phong model, of the new model and of real metal mirrors at grazing angles*

7.2. Coated metals, metallic paints

We concluded that the new model is not a perfect metallic model because the BRDF of metals goes to infinity at grazing angles while the BRDF of the new model is bounded but its reflection lobe gets wider in order not to absorb all energy. Considering real materials, metals coated by a lacquer layer[21] behave like this. Since in lacquer the attenuation of the power is an exponential function of the length travelled, for higher incident angles, both the reflected radiance and power will tend to zero at grazing angles. If the lacquer also contains the particles of the basic metal, then the behaviour of the material will be in between the metal and lacquered metals. Absorption, scattering and reflection can occur simultaneously in the lacquer layer. Thus for higher incident angles the metal particles, especially those that are close to the surface, will be responsible for reflecting the incoming photons. The object acts as energy mirror even if the reflected radiance decreases. Consequently the new model seems

s	$C_{\max}$	$I_{1,2}$	a_{Diffuse}	
0	$1/\pi$	0	1	LAMBERTIAN
0.25	0.3754	0.20316	0.71527	
0.5	0.4411	0.33071	0.50979	
1.	0.6023	0.44002	0.25608	
2	1.0718	0.39401	0.06167	
4	2.8032	0.15834	0.00295	
8	10.216	0.01076	0.00000	
16	40.743	0.00001	0.00000	HIGHLY SPECULAR
32	162.97	0.00000	0.00000	
64	651.89	0.00000	0.00000	
128	2607.5	0.00000	0.00000	
256	10430.	0.00000	0.00000	
512	41721.	0.00000	0.00000	ALMOST MIRROR

Table 1: *Parameters of the* $f_r = C_{\max} \cdot e^{-s \cdot m}$ *BRDF*

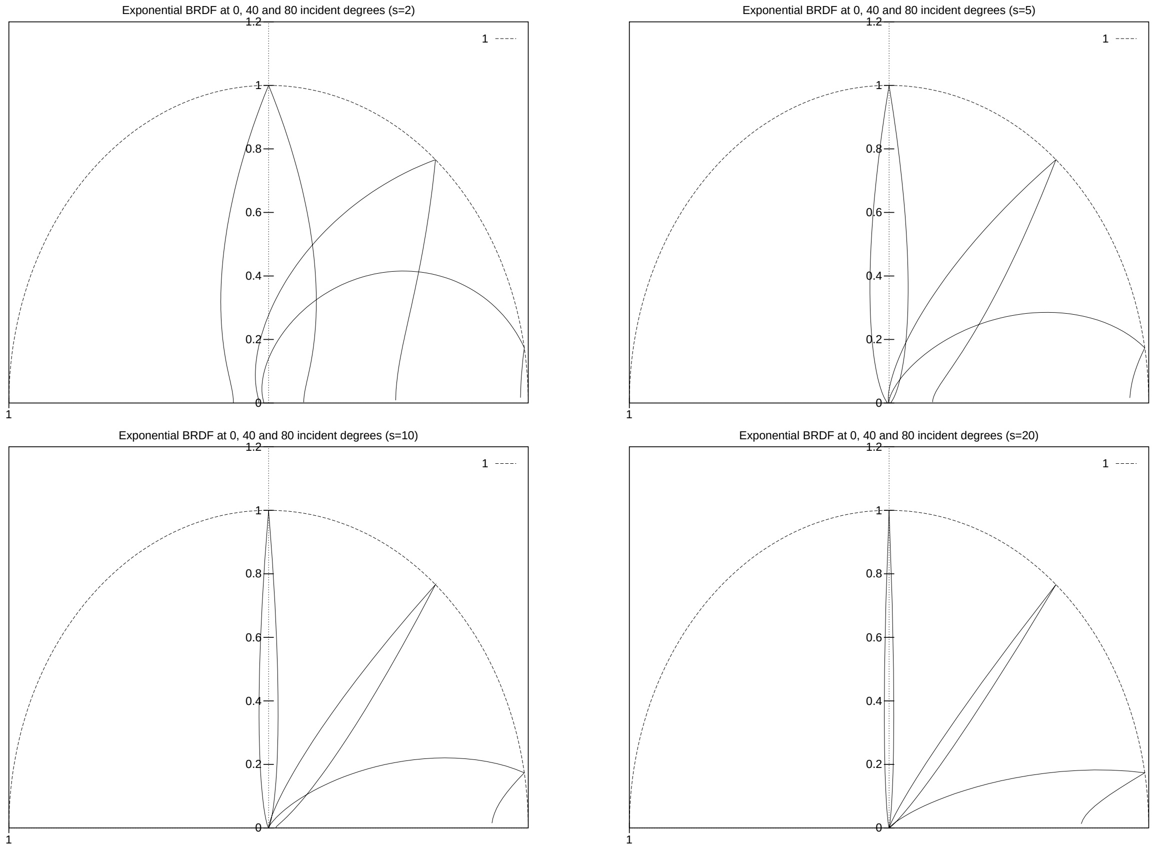

Figure 17: *BRDF using exponential weight function*

to be appropriate for representing coated metals and metallic paints.

Since the diffuse component of the metals is practically negligible, the metallic paints are approximated as follows

$$C_{\max} \cdot \xi(m) \cdot \mathrm{Fresnel}(\theta'), \qquad (51)$$

where $C_{\max} \cdot \xi(m)$ is a BRDF. For metals, the $\xi(m)$ function has a quite small diffuse component. We can use, for example, the $\xi(m) = (s^2/2\pi) \cdot e^{-s \cdot m}$ function, assuming that $s > 10$.

The wavelength dependent Fresnel function describes the reflection of the optically smooth material as a function of the incident angle.

In the Cook-Torrance model, as well as in other mirror-particle models, for a given $(\mathbf{L}, \mathbf{V})$ pair, the expectation of the normal vectors of the reflecting facets is the $\mathbf{H}$ vector, thus the angle of incidence is $\theta_{\mathbf{H}} = \arccos(\mathbf{N} \cdot \mathbf{H})$.

This approach is slightly modified in the following way. The distance of the $\mathbf{H}_P = (\mathbf{V}_P + \mathbf{L}_P)/2$ vector from the $\mathbf{O}$ origin is used to evaluate the Fresnel function.

$$|\mathbf{H}_P - \mathbf{O}| = \frac{|\mathbf{L}_P - \mathbf{V}_P|}{2} = \frac{|\mathbf{g} - (\mathbf{N} \cdot \mathbf{g})\mathbf{N}|}{2} = \frac{m(\mathbf{L}, \mathbf{V})}{2}. \qquad (52)$$

where the $m(\mathbf{L}, \mathbf{V})$ metric is described by formula (29) belonging to the retro-reflective model.

Let us define angle θ' in the following way:

$$\theta' = \arcsin\left(\frac{m(\mathbf{L}, \mathbf{V})}{2}\right). \qquad (53)$$

In conclusion, the proposed new model is:

$$f_{r,\mathrm{metallic}}(\mathbf{L}, \mathbf{V}) = \frac{s^2}{2\pi} \cdot e^{-s \cdot |\mathbf{h} - (\mathbf{N} \cdot \mathbf{h})\mathbf{N}|} \cdot \mathrm{Fresnel}_\lambda(\theta'). \qquad (54)$$

where $\theta' = \arcsin(|\mathbf{g} - (\mathbf{N} \cdot \mathbf{g})\mathbf{N}|/2)$.

The model is the product of a reflective and a retro-reflective model. Importance sampling can be performed efficiently on the reflective factor, the retro-reflective factor modifies the weights of the elementary rays as a multiplier.

7.3. Plastics and polishing

Using a real refraction index in the Fresnel term instead of the complex index of metals, the proposed model can also be used for modelling the specular reflection of plastics. Since the diffuse reflection of plastics is also significant, the BRDF function is defined as a sum of the diffuse and specular terms. To meet the requirement of energy conservation, the sum of the albedos of the diffuse and specular part must be less than 1. The BRDF is then

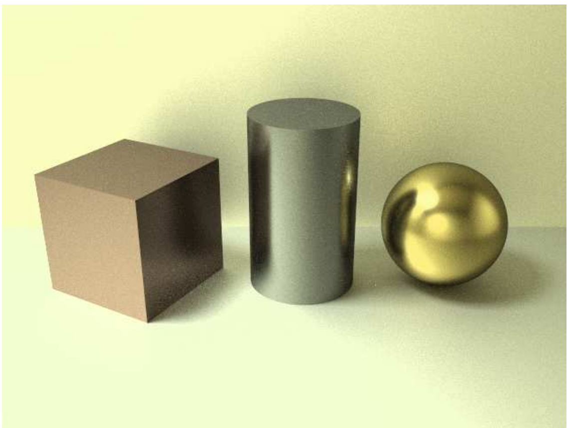

Figure 19: *A simple scene with a cube ($s = 2$) cylinder ($s = 4$) and sphere ($s = 8$)*

$$f_{r,\mathrm{plastics}} = \frac{a_{\mathrm{diffuse}}}{\pi} + (1 - a_{\mathrm{diffuse}}) \cdot C_{\max} \cdot \xi(m) \cdot \mathrm{Fresnel}(\theta'). \qquad (55)$$

Certain materials, as for example lacquered objects, reflect sharp mirror images for large viewing angles [13]. To simulate this phenomenon, any of the proposed BRDFs can be supplemented by an ideal mirror in the following way:

$$f_{r,\mathrm{mirrorextension}} = f_r(\mathbf{L}, \mathbf{V}) + (1 - a(\mathbf{L})) \cdot f_{r,\mathrm{idealmirror}}(\mathbf{L}, \mathbf{V}). \qquad (56)$$

Note that the extension is limited by the "missing albedo" of the original BRDF. The BRDF of the ideal mirror is a Dirac function:

$$f_{r,\mathrm{idealmirror}}(\mathbf{L}, \mathbf{V}) = \frac{\mathrm{Fresnel}(\theta') \cdot \delta(\mathbf{L}' - \mathbf{V})}{\cos\theta}. \qquad (57)$$

7.4. Generalised Lambertian models

The $\xi(m)$ function can be monotone increasing as well. In this case the reflected radiance will have smaller slope as the incident angle changes than the cosine function obtained from the Lambertian model, which conforms to the measurements using a certain class of materials, including ceramic, wall, foam, cloth, etc. Due to the local interreflections - especially for great incident angles - these materials reflect more light backwards, than forwards in the mirror direction.

Oren et. al.[11] also proposed a model for these types of materials. Here a different approach is presented. To obtain such a model, let us assume that the light source is placed in the viewpoint. An appropriate function of the reflected radiance that has a "smoother" slope than the Lambertian model is $\cos^{1-d}\theta$ where θ

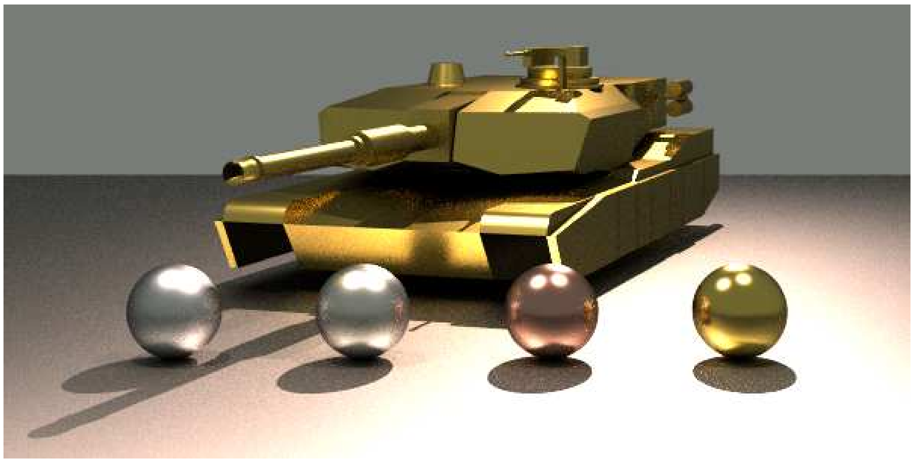

Figure 18: *Scene rendered using Russian roulette including a golden tank ($s = 10$), silver base plane ($s = 4$), aluminium ($s = 6$), silver ($s = 8$), copper ($s = 15$) and golden ($s = 20$) spheres*

is the angle of the light and of the normal vectors and d is the smoothness parameter. In the limit case of $d = 0$ the diffuse case is obtained, for the $d = 1$ limit case we get a disk of constant radiance, which is like the full moon. This selection leads to the following ξ function:

$$\xi(m) = \left(1 - \left(\frac{m}{2}\right)^2\right)^{-d/2}, \qquad 0 \le d \le 1. \tag{58}$$

Unfortunately, these models do not satisfy the principle of the conservation of energy, so we have to modify definition (58). The simplest way of correcting this is to limit the BRDF with a constant. Another possible approach is to consider the MacLaurin's series of the function, retaining only a few terms, such that the truncated series will be less than the original function.

As an example, let us consider the case when the function is clipped by a constant:

$$f_r(\mathbf{L}, \mathbf{V}) = C_{\max} \cdot \min\left(\left(1 - \left(\frac{m}{2}\right)^2\right)^{-d/2}, \xi_{\max}\right), \tag{59}$$

where $0 \le d \le 1$.

Table 3 has been generated using a clipping where the function was taken to be constant above $m = 1.9$, that is $\xi_{\max} = \xi(1.9)$. The $C_{\max}$ value was determined such that the maximum value of the albedo is 1. For the above model, this is reached always for $m = 2$. The minimum of the albedo is always in $m = 0$. So, contrary to the case of monotone decreasing functions, the pure diffuse component is defined by the case corresponding to $m = 0$.

The model defined by formula (59) can always be described as the sum of a Lambertian model with an albedo (reflectivity) of a_{Diffuse} and of a complementary model. The albedo of the latter is zero for $m = 0$ and it is a monotone increasing function of m. Formula (59) has the same behaviour as the model defined by equation (58), except for the $m > 1.9$ domain. In the case of $1.9 \le m \le 2$, the reflected radiance for the above mentioned sphere will have a decrease proportional to the cosine function at $[0, 1]$.

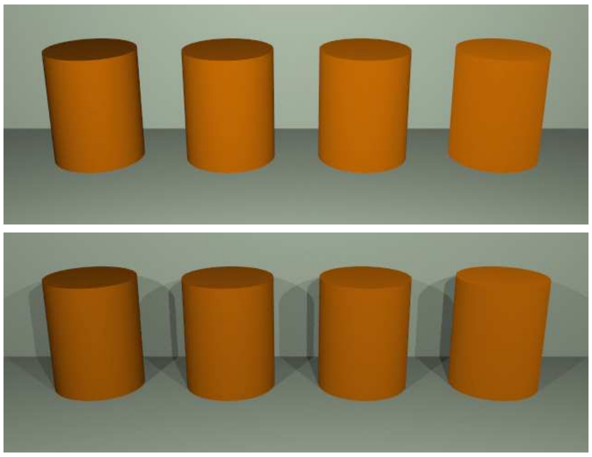

Figure 20: *Objects ($d = 1$, $d = 0.75$, $d = 0.5$, $d = 0.25$) rendered using generalised Lambertian BRDFs computing only the direct illumination effects. In the upper image the light source is at the view position, in the lower image there are two point light sources*

The "full moon" limit case means that for a sphere

d	$C_{\max}$	$f_{\max}$	a_{diffuse}	
0	$1/\pi$	1.0	1.0	LAMBERTIAN
0.1	0.30884	1.123440	0.97689	
0.2	0.29939	1.262117	0.95352	
0.3	0.28998	1.417912	0.92989	
0.4	0.28061	1.592939	0.90602	
0.5	0.27128	1.789571	0.88193	
0.6	0.26200	2.010475	0.85764	
0.7	0.25278	2.258647	0.83318	
0.8	0.24363	2.537454	0.80856	
0.9	0.23456	2.850676	0.78381	
1.0	0.22556	3.202563	0.75895	"FULL MOON"

Table 3: *Parameters obtained for the generalised Lambertian model*

illuminated from the viewpoint the radiance will be constant, only at the margins will decrease with a cosine character. The width of the "cosine-ring" can be controlled by modifying $\xi_{\max}$. It is advisable to choose the value of d in formula (59) to be less than 1.

For the above model, a good approximation of the importance sampling is to generate directions (with a "cosine" distribution) like in the case of the Lambertian model and to use an appropriate multiplier correction factor for each ray.

8. Conclusions and future work

The paper presents a new, simple and unified definition for obtaining a good visual approximation for many materials. The new model class can be used easily in the majority of the commercial programs. By allowing the interactive definition of the $\xi(m)$ highlight profile functions, BRDF characteristics can be specified in a new manner.

Due to their simplicity, the computation cost of the new models is low. According to our running time measurements using Heckbert's BRDF viewer[22], the computational time of the new model is practically equal to the time of the Phong-Blinn model and half of the time of the Ward model. Importance sampling, on the other hand, is simpler and faster for the new model than for previous models.

One of the problems to be solved by further research is to investigate which of the physically plausible BRDFs (fulfilling reciprocity, energy conservation and non-negativity) can be defined by suitable

$$(T(\mathbf{L}), m(\cdot,\cdot), p(R))$$

triplets (see section 5). Another important question is which materials can be modelled as the sum, product and other generalisations of the introduced reflective and retro-reflective models.

9. Acknowledgements

This work has been supported by the National Scientific Research Fund (OTKA ref.No.: F015884, T029135) and the Austrian-Hungarian Action Fund (ref.No.: 29ö4 and 32öu9). The authors thank Eric Lafortune for the implementation of the generalised Lambertian model and for the rendering of images 19 and 20, and Paul Heckbert for providing his BRDF editor which has been extended and used to create the BRDF curves.

References

1. R. Lewis. Making shaders more physically plausible. In *Rendering Techniques '93*, pages 47–62, 1993.
2. P. Beckmann and A. Spizzichino. *The Scattering of Electromagnetic Waves from Rough Surfaces.* MacMillan, 1963.
3. K. Torrance and M. Sparrow. Off-specular peaks in the directional distribution of reflected thermal distribution. *Journal of Heat Transfer — Transactions of the ASME*, pages 223–230, May 1966.
4. R. Cook and K. Torrance. A reflectance model for computer graphics. *Computer Graphics*, 15(3), 1981.
5. X. He, K. Torrance, F. Sillion, and D. Greenberg. A comprehensive physical model for light reflection. *Computer Graphics*, 25(4):175–186, 1991.
6. J. T. Kajiya. Anisotropic reflection models. In *Computer Graphics (SIGGRAPH '85 Proceedings)*, pages 15–21, 1985.

7. G. Ward. Measuring and modeling anisotropic reflection. *Computer Graphics*, 26(2):265–272, 1992.

8. B. T. Phong. Illumination for computer generated images. *Communications of the ACM*, 18:311–317, 1975.

9. J. F. Blinn. Models of light reflection for computer synthesized pictures. In *Computer Graphics (SIGGRAPH '77 Proceedings)*, pages 192–198, 1977.

10. T. Whitted. An improved illumination model for shaded display. *Communications of the ACM*, 23(6):343–349, 1980.

11. M. Oren and S. Nayar. Generalization of Lambert's reflectance model. *Computer Graphics (SIGGRAPH '94 Proceedings)*, pages 239–246, 1994.

12. J. Beard and J. R. Maxwell. Bidirectional reflectance model validation and utilization. Technical Report AFAL-TR-73-303, 1973.

13. E. Lafortune, S. Foo, K. Torrance, and D. Greenberg. Non-linear approximation of reflectance functions. *Computer Graphics (SIGGRAPH '97 Proceedings)*, pages 117–126, 1997.

14. L. Neumann and A. Neumann. A new class of brdf models with fast importance sampling. Technical Report TR-186-2-96-24, Institute of Computer Graphics, Vienna University of Technology, 1996. www.cg.tuwien.ac.at/.

15. R. F. Tobler, L. Neumann, M. Sbert, and W. Purgathofer. A new form factor analogy and its application to stochastic global illumination algorithms. In *Rendering Techniques '98*, 1998.

16. D. S. Immel, M. F. Cohen, and D. P. Greenberg. A radiosity method for non-diffuse environments. In *Computer Graphics (SIGGRAPH '86 Proceedings)*, pages 133–142, 1986.

17. E. Lafortune and Y. D. Willems. Using the modified phong reflectance model for physically based rendering. Technical Report RP-CW-197, Department of Computing Science, K.U. Leuven, 1994.

18. L. Neumann and A. Neumann. Radiosity and hybrid methods. *ACM Transactions on Graphics*, 14(3):233–265, 1995.

19. L. Szirmay-Kalos. *Theory of Three Dimensional Computer Graphics*. Akadémia Kiadó, Budapest, 1995. http: //www.iit.bme.hu/˜szirmay.

20. Ch. Schlick. A customizable reflectance model for everyday rendering. In *Fourth Eurographics Workshop on Rendering*, pages 73–83, Paris, France, 1993.

21. L. Neumann and A. Neumann. Photosimulation: Interreflection with arbitrary reflectance models and illumination. *Computer Graphics Forum*, (8):21–34, 1989.

22. P. Heckbert. Brdf viewer. 1997. http: //www.cs.cmu.edu/afs/cs.cmu.edu/user/ph/ www/src/illum.

23. P. Poulin and A. Fournier. A model for anisotropic reflection. *Computer Graphics*, 24(4):273–281, 1990.

24. M. Minnaert. The reciprocity principle in lunar photometry. *Astrophysical Journal*, 93:403–410, 1941.

25. E. Ken. Reflectance phenomenology and modeling tutorial. 1994. http://www.erim.org.

26. B. Hapke. A theoretical photometric function for the lunar surface. *Journal of Geophysical Research*, 68(15), 1963.

27. R. Hall. *Illumination and Color in Computer Generated Imagery*. Springer-Verlag, New York, 1989.

28. I. Deák. *Random Number Generators and Simulation*. Akadémia Kiadó, Budapest, 1989.

29. L. Neumann, A. Neumann, and L. Szirmay-Kalos. New simple reflectance models for metals and other specular materials. Technical Report TR-186-2-98-17, Institute of Computer Graphics, Vienna University of Technology, 1998. www.cg.tuwien.ac.at/.

30. L. Neumann, A. Neumann, and L. Szirmay-Kalos. Analysis and pumping up the albedo function. Technical Report TR-186-2-98-20, Institute of Computer Graphics, Vienna University of Technology, 1998. www.cg.tuwien.ac.at/.

31. L. Neumann, A. Neumann, and L. Szirmay-Kalos. Compact metallic reflectance models. *Computer Graphics Forum (Eurographics'99)*, 18(3):161–172, 1999.

32. L. Neumann, A. Neumann, and L. Szirmay-Kalos. Reflectance models by pumping up the albedo function. *Machine Graphics and Vision*, 8(1):3–18, 1999.